EUROFUSION WPJET3-PR(15) 14330

P Batistoni et al.

On the absolute calibration of neutron measurements in fusion reactors

Preprint of Paper to be submitted for publication in
Fusion Engineering and Design

This work has been carried out within the framework of the EUROfusion Consortium and has received funding from the Euratom research and training programme 2014-2018 under grant agreement No 633053. The views and opinions expressed herein do not necessarily reflect those of the European Commission.

On the absolute calibration of neutron measurements in fusion reactors

P. Batistoni[1]

[1] *ENEA Fusion and Nuclear Safety Technology Department, Via E. Fermi 45, I-00044 Frascati (Rome), Italy*

This paper focuses on the issues of obtaining and maintaining the absolute calibration of neutron measurements in fusion reactors, including also ITER and DEMO. Such absolute calibration is required to provide the fusion power, to account for burnt Tritium, and to derive plasma ion parameters. The usual calibrating procedure adopted so far in fusion devices appears to be very complex already when applied in ITER, and most probably unviable in DEMO and in the future power plants. An alternative solution based on the neutron activation technique using long-lived radioisotopes is proposed in this paper. Potential reactions are investigated and the expected activity levels are calculated for several materials in ITER. A test in JET is proposed.

Keywords: fusion reactor, neutron measurements, absolute calibration, fusion power

1. Introduction

An accurate absolute calibration of neutron detectors is required in fusion reactors as they provide a measurement of the fusion power and of the Tritium burnt in fusion reactions, which must be known for Tritium accountancy, as well as other plasma parameters. The usual procedure adopted so far in fusion devices to calibrate neutron detectors is based on recording neutron detector signals when a calibrating neutron source of known intensity is deployed inside the machine at different toroidal and poloidal locations [1,2,3]. Generally, ^{252}Cf neutron sources and DT neutron generators have been used to calibrate neutron detectors at 2.5 MeV and 14.1 MeV energy, respectively [1,2]. Numerical simulations are used to estimates the effects of different circumstances of calibration as compared to the plasma volumetric source, due to the discrete positions and to different energy spectrum and angular emission distribution of calibrating (point) sources.

Most fusion experiments employ both active detectors located around the machine (fission chambers, proportional counters, scintillators etc..) to monitor the time evolution of the neutron emission rate, and activation systems which allow for a transfer of activation samples inside the machine and their removal, for instance on a shot by shot basis. Activation systems employ encapsulated foils pneumatically transferred from the in-vessel irradiation stations to the gamma-ray measurement station where the neutron-induced activity is measured. This system provides an absolute measurement of the local neutron fluence at the irradiation station during the irradiation time, which can be related to the total neutron yield in the same time interval by radiation transport calculations. Provided that the irradiation stations are sufficiently close to the first wall, and high-energy threshold activation reactions are used, the activation system can be considered to respond mostly to direct neutrons. However, detailed numerical calculations can provide the correct response including the contribution due to scattered neutrons.

Active detectors, fully characterized in the laboratory, respond only to the local neutron field, which is determined by radiation transport in the tokamak and in the detector itself. The materials, especially those between the neutron source and detector positions, cause neutron flux attenuation and affect the neutron spectrum. Usually, detectors do not distinguish between direct and scattered neutrons, and this is why in situ calibration of detectors complemented with neutron transport calculation are necessary.

The absolute calibration of neutron detectors in fusion systems is becoming more difficult as the size of devices increases, requiring calibrating sources of higher intensity and longer irradiation times. Recently, a new neutron calibration has been carried out at JET (after 24 years from the previous one) based on the use of a ^{252}Cf source with intensity equal to 2.7×10^8 n/s deployed inside the vacuum vessel in more than 200 toroidal/poloidal positions in two weeks by means of the JET remote handling boom [4]. A new calibration at 14 MeV neutron energy is being prepared in preparation of the new DT operations planned for 2019 [5]. It will use a DT neutron generator calibrated and characterized in laboratory before the in-vessel calibration.

In ITER, a comprehensive set of neutron detectors will be installed and will be calibrated through a complex calibration strategy [6]. The neutron diagnostics will allow evaluation of the neutron emissivity, i.e. the fusion power, and will play a key role for machine protection as well for plasma optimization and for achieving ITER goals, in particular the target fusion gain factor, Q. ITER expected neutron emission strength spans over 7 decades (from 10^{14} up to almost 10^{21} n/s). The various neutron diagnostic systems will have to be able to measure the neutron emissivity within 10% accuracy, with a temporal resolution of 1 ms and spatial resolution of a tenth of the minor plasma radius, i.e. 200 mm. These include neutron flux monitors (fission chambers coated with varying amount of ^{235}U and ^{238}U fissile material) installed in diagnostic ports and below the divertor dome, ^{235}U micro-fission chambers deployed between the blanket modules and the inner shell of the vacuum vessel, and the radial and vertical neutron cameras. A Neutron Activation System (NAS) will also be installed with irradiation ends inside the vacuum vessel.

It is planned to apply the in situ calibration also to ITER neutron detectors. A powerful DT neutron generator - with intensity $\sim 10^{10}$ - is needed and will have to be developed. This intensity is, however, many orders of magnitude lower than the plasma neutron intensity, and the huge differences in neutron flux the detectors experience during the ITER operations as compared to the calibration procedures requires many cross calibration steps. The use of a DT neutron generator introduces additional sources of uncertainties in the calibration as compared to ^{252}Cf sources. The characteristics of DT neutron sources, in fact, are very complex functions of energy and emission angle, which need to be carefully charaterised and calibrated before they can be reliably used as calibration sources. Given the neutron emission intensity required, the neutron generator itself will be massive and will have to incorporate a cooling system. Account needs to be taken of the potential screening and scattering effects of the structure that will support the neutron source by means of neutron transport code calculations. In ITER it is estimated that it will take eight weeks at least with this source to calibrate flux monitors, profile monitors, and the activation system [7]. Full in-situ calibration experiments are planned only before the beginning of the ITER nuclear phase. During ITER life the characteristics of the detectors may vary due to environmental changes. These changes have to be tracked by measurements using weak neutron sources, and cross-calibration with activation measurement using reference discharges (long-term and periodic calibration) [8].

Therefore, the activation system plays a fundamental role in the ITER neutron calibration strategy because it is the only neutron diagnostic having a dynamic range of many orders of magnitude thanks to appropriate selection of mass and foil materials. However, high thermal loads are expected at the irradiation ends because of the plasma radiation and nuclear heating. This fact precludes a number of

materials for the capsule or sample, such as polyethylene, In and Al, and in any case active cooling is needed, introducing complexity in the system design. EM forces induced by plasma disruptions require the design of dedicated strong supports. R&D activity is on-going on the selection of material and mass of the samples. The location of irradiation ends has to take into account a number of constraints that prevent an optimal positioning to be obtained. The optimal location would be as close as possible to the first wall, with a complete view of the emitting plasma and in the absence of collimating effects. In ITER, several irradiation stations will be positioned between various blanket modules and on the vessel inner wall as well in the Upper and Equatorial Ports.

The implementation of diagnostics systems in DEMO and in future power plants will be even more challenging and will require a new and very pragmatic approach. This will be true in particular for neutron diagnostics that will be undeniably essential. Activation systems with the current design, i.e. with irradiation ends close to the first wall, will be most probably unviable in DEMO and in future power plants, for which new concepts for neutron diagnostics will have to be developed. Proposals have been made of using the activation of circulating water in a dedicated loop as a fusion monitor in future fusion reactors. The method is based on the measurement of the $^{16}O(n,p)^{16}N$ reaction that has a threshold energy of 10.4 MeV [9].

An alternative solution for DEMO, based on the complementary use of the neutron activation technique employing long exposure times and using long-lived radioisotopes together with short lived ones, is proposed in this paper and aims at providing a periodic calibration of neutron detectors along the reactor lifetime. This proposed solution partially disentangles the problem of accurate absolute calibration from the time resolved measurement of fusion power, and requires a first, dedicated nuclear phase of operations devoted to calibration of the activation system at the beginning of the reactor life. This approach should be tested in ITER. Potential reactions are investigated and the expected activity levels are calculated for several materials in the ITER case. A test in JET is proposed.

2. A new calibration approach

The proposed approach aims at providing a first, and then a periodic, calibration of time resolved neutron monitors, and is based on the use of activation samples, made of suitable metals, attached to in-vessel components (or sub-components) that are expected to be refurbished/replaced at a frequency of a few years, such as the divertor cassettes, port plugs or blanket modules. The samples will have to be located close to the plasma facing side of such components so that they are exposed to fusion neutrons and, at the same time, protected from direct plasma interactions. The system, which we will call Long term Neutron Activation System, L-NAS, would involve simple attachment of very small samples (a few grams) not requiring any dedicated cooling system. A second, 'traditional' activation system with pneumatic transport of samples at irradiation ends, and employing activation reactions producing radioisotopes with both long and relatively short half-lives (S-NAS), would be cross calibrated with the L-NAS and would record neutrons with a desired time resolution (one discharge or a few days, or weeks).

2.1 Theoretical background

Activation reactions generating suitably long-lived radioisotopes will have to be employed so that the neutron induced radioactivity measured after the foil removal could be related to the total neutron fluence at the sample during the irradiation period, which in turn is related to the neutron yield in the same time interval.

The net production rate of radioisotope N_j is given by

$$\frac{dN_j(t)}{dt} = N_i \equiv_E {}_{ij}(E) \quad (E,t)dE \qquad {}_jN_j(t) \qquad (1)$$

where N_i is the number of parent (stable) isotopes in the sample, $\Phi(E,t)$ is the neutron flux density, E is the neutron energy, $\sigma_{ij}(E)$ is the cross section of the reaction $N_i(n,X)N_j$, λ_j is the decay constant of radioisotope N_j, i.e. the inverse of the decay time $\lambda_j = ln2/\tau_{1/2}$, $\tau_{1/2}$ being the half life.

The local neutron flux density is proportional to the total neutron yield $Y(E,t)$ by a factor $C(E,t)$ which takes into account the neutrons source space and energy distribution, the reactor geometry and materials, and the sample location.

$$(E,t) = Y(E,t)C(E,t) \qquad (2)$$

$C(E,t)$ is calculated by neutron transport calculations. Though $C(E,t)$ could be in principle depend on time, it could be assumed to be constant provided that the reactor in-vessel configuration and materials are not modified in time.

If we assume a constant neutron flux density for simplicity, which would be produced by a constant neutron yield, after a time t from the start of exposure but still during irradiation, i.e. at $t < T_{irr}$, where T_{irr} is the end of irradiation time, the number of radioisotopes produced in the sample is

$$N_j(t) = \frac{N_i}{\lambda_i}\left(1 \quad e^{\lambda_j t}\right) \equiv_E \sigma_{ij}(E) \quad (E)dE \qquad (3)$$

$$A_j(t) = \lambda_j N_j(t) = N_i\left(1 \quad e^{\lambda_j t}\right) \equiv_E \sigma_{ij}(E) \quad (E)dE \qquad (4)$$

In the two limiting cases of large or small decay constants (short and long decay times), the activity is given by

$$\begin{aligned} &a) \quad \frac{1}{\lambda_j} << t < T_{irr} \qquad A_j(t) \oplus N_i \equiv_E (E)\sigma_{ij}(E)dE \\ &b) \quad t < T_{irr} << \frac{1}{\lambda_j} \qquad A_j(t) \oplus N_i\lambda_j t \equiv_E (E)\sigma_{ij}(E)dE \end{aligned} \qquad (5)$$

In the first case of short decay times, the activity saturates at a level given by the neutron flux density and does not increase with continuing irradiation. In the second case of long decay times, the activity increases with time. In this last case, the activity at the end of irradiation is a function of the total neutron yield produced during the irradiation time. As the activity is proportional to λ_j, however, large decay times are in principle not advantageous. Therefore, suitable activation reactions should be characterized by a decay time comparable to a typical irradiation time, here assumed to be of the order of a few years.

$$\lambda_j \oplus \frac{1}{T_{irr}} \qquad (6)$$

In general, after the end of irradiation, $t > T_{irr}$, the activity is given by

$$A_j(t) = N_i\left(1 - e^{-\lambda_j T_{irr}}\right)e^{-\lambda_j t}\int_E \sigma_{ij}(E)\,\Phi(E)dE = A(T_{irr})e^{-\lambda_j t} \qquad (7)$$

where $A(T_{irr})$ is the activity at the end of irradiation.

During reactor operation the neutron emission would not be constant and its time profile needs to be taken into account. The complete expression for $A(T_{irr})$ is

$$A_j(T_{irr}) = N_i\left(1 - e^{-\lambda_j T_{irr}}\right)\int_{t'=0}^{T_{irr}}\int_E \sigma_{ij}(E)\,\Phi(E,t)dE = N_i\left(1 - e^{-\lambda_j T_{irr}}\right)Y(T_{irr})\int_{t'=0}^{T_{irr}}\int_E \sigma_{ij}(E)f(t)C(E,t)dEdt \qquad (8)$$

where $Y(T_{irr})$ is the total neutron yield produced during the irradiation time (neglecting its dependence on energy), $f(t)$ is the time profile of the neutron emission during the irradiation time and $C(E,t)$ describes the variation in time of the local neutron flux density which may be due to plasma position and shape variations, energy spectrum variation.

Provided that N_i, $\sigma_{ij}(E)$ and λ_j are well known, and that $f(t)$ can be obtained from time resolved neutron counters (provided that they are stable, see discussion below), then $Y(T_{irr})$ can be calculated from the measurement of $A_j(T_{irr})$. The variation in time of the plasma position and shape would probably not be easily available from other measurements but, on one hand, we cannot expect much departure from the standard plasma scenario in DEMO and power plants and, on the other hand, the use of activation foils at different poloidal angles can provide the weighted average position of the neutron emission centre, as discussed later in §3.2. This method can be used for periodic calibration of neutron detector monitors.

The neutron activation technique has been largely used as a neutron diagnostic method in many tokamaks. It has generally made use of activation reactions producing short-lived radioisotopes so to be able to measure the absolute neutron production rate with some time resolution, on a shot-by-shot basis or less, and to allow to reuse foils in subsequent shots after the activity had completely decayed. The most generally used reactions for DD neutrons are the ^{115}In(n,n')^{115m}In reaction ($\tau_{1/2}$ = 4.486 h), the ^{238}U(n,f) reaction ($\tau_{1/2} \approx$ 1 min), and ^{232}Th(n,f) reaction ($\tau_{1/2} \approx$ 1 min). For DT plasmas, the ^{28}Si(n,p)^{28}Al ($\tau_{1/2}$ = 2.24 min), ^{27}Al(n,p)^{27}Mg ($\tau_{1/2}$ = 9.458 min), ^{63}Cu(n,2n)^{62}Cu ($\tau_{1/2}$ = 9.74 min), and ^{56}Fe(n,p)^{56}Mn ($\tau_{1/2}$= 2.58 h) reactions have been used.

2.2 Proposed method

The method proposed here is based on the use of two combined Neutron Activation Systems.

A Long term Neutron Activation System, L-NAS, consisting of very small samples (a few grams) attachable and removable by remote handling on in-vessel components (or sub-components) that are expected to be refurbished or replaced at a frequency of a few years. L-NAS should not require any dedicated cooling system. The employed activation reactions would produce long lived radioisotopes, i. e. with half-lives of the order of the duration of a full operation campaign between two subsequent (planned) shutdowns. The activation measurements would provide the local neutron fluence at the foil position. Numerical analyses would be needed in order to calculate C(E,t) and derive the neutron yield from the local fluence. Apart from the numerical uncertainties, which are expected to be small in the case of samples located close to the first wall and using high threshold cross sections, as discussed in the Introduction, more than one poloidal positions would be desirable for L-NAS.

The method relies also on the combined use of a 'traditional' activation system with pneumatic transport of samples at irradiation ends and employing activation reactions producing radioisotopes with both long and relatively short half-lives (S-NAS), which would record neutrons with a desired time resolution (one discharge or a few days, or weeks). This 'traditional' activation system, however, does not necessarily need to expose foils close to the first wall, and would be located in more external reactor regions less prone to nuclear heating or radiation damage. S-NAS would be cross-calibrated with respect to the long term one (L-NAS). The potential locations of the S-NAS in a tokamak reactor are on the vacuum vessel behind the bulk shield, avoiding exposure along neutron streaming paths, on positions where any dedicated cooling system would not be necessary and the neutron induced damage to materials would be limited (Fig.1).

The characteristic of this method is that it disentangles the measurement of the absolute neutron yield from that of its time profile. The total absolute neutron yield measurement is periodically obtained at shutdowns with in-vessel interventions when the L-NAS foils would be available, and is used *a posteriori* to calibrate the time-resolved neutron monitors. An implicit assumption is that the inner tokamak components would not be modified during the reactor lifetime.

2.3 Time drift of the efficiency of the time-resolved neutron monitors

The proposed method disentangles the problem of accurate absolute calibration from time resolved measurement of power. The total absolute neutron yield measurement is obtained when the foils are accessible and is used *a posteriori* to calibrate the time-resolved neutron monitors. The time variation of fusion power, however, has to be monitored to provide the $f(t)$ time profile function in Eq.8 . However, the efficiency of neutron monitors may vary in time and this is precisely why a periodic calibration is needed. We have already seen that any drift in time in the efficiency of the time-resolved neutron monitors occurring during the previous operations would result in a wrong calibration of these detectors.

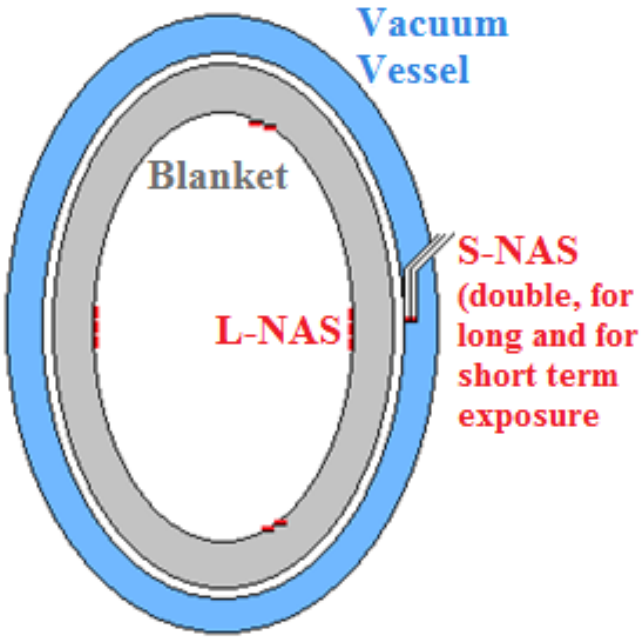

Fig. 1 Sketch showing the principle of the proposed method with potential position of L-NAS and of S-NAS

The solution to this issue relies on the combined use of L-NAS and S-NAS, with S-NAS providing verification of constant ratio of S-NAS activation with active neutron monitors response. For this purpose, the S-NAS should consist of couples of identical irradiation ends located in the same position: one would be used for short irradiations to monitor the stability of neutron monitors, the second one would be used for long irradiations (same time interval as L-NAS) and would be periodically cross-calibrated with the L-NAS (Fig.1). The active neutron monitors in ITER and in DEMO will consist of many detectors with different sensitivities in order to cover the neutron emission rate range of many orders of magnitude. The combined L-NAS and S-NAS system would provide an absolute and unique calibration method of neutron monitors over the required range, from DD operations to high performance DT operations.

L-NAS and the S-NAS irradiation ends devoted to cross calibration for L-NAS could use the same activation reactions to reduce the propagation of measurement errors. However, if needed in order to extend the applicable neutron emission rate range, other reactions could be used in S-NAS (where the neutron fluence would be lower by a few orders of magnitude than in LNAS), characterized by much higher cross section values, such as (n,γ) neutron capture reactions, as discussed later in §3.2. In fact, the use of high-energy threshold reactions is necessary only in the L-NAS.

2.4 Need of an initial calibration of neutron monitors and discrimination of DD and DT neutrons

The proposed system can provide calibration of external neutron monitors only when the L-NAS samples are removed in the first shutdown with in-vessel intervention after the start of the nuclear phase. However, calibration of neutron monitors is needed soon at the start of the nuclear phase.

In order to obtain it, a first operation, even with Deuterium plasma only, should be devoted to initial calibration. During this phase, the activation foils would be exposed in the L-NAS for the first time. In this phase, a preliminary calibration of neutron monitors would be based on short-lived activation measurements at S-NAS combined with the calculation of neutron spectra at its irradiation ends. Based on the experience gained on a number of neutron benchmark experiments with 14 MeV neutrons, a target accuracy of ≈ 20% would be achieved for this preliminary calibration, provided that the S-NAS is behind no more than about 1 meter of shield made of a combination of typical blanket materials (stainless steel, water, Be, Li or LiPb) from the first wall [10], and provided that the local geometry and materials are well known.

At the end of this initial phase, both $Y_{tot} = Y_{DD} + Y_{DT}$ and Y_{DT} total neutron yields (the latter from triton burnup) can be measured separately by L-NAS by employing reactions of different energy thresholds E_{th}, for example $E_{th,tot} > 1.5$ MeV and $E_{th,DT} > 5$MeV, respectively (see Table 1). A first calibration of the external neutron monitors can then be obtained using L-NAS only. If an accurate calibration of the L-NAS and the S-NAS systems is also desired, a minimum neutron yield is needed as discussed later in §3.2,

Whereas the cross calibration factors for DT neutrons between S-NAS and L-NAS will remain constant with varying Y_{DT}/Y_{DD} yield ratios in subsequent operation phases, this is not true for the cross calibration for the total yield Y_{tot}. In pure Deuterium plasmas DT neutrons arise from the burn-up of tritons produced in DD reactions, Y_{DT}/Y_{DD} being typically equal to a few per cent. In DT plasmas, $Y_{DT}/Y_{DD} \approx 200$ due to the difference between the DT and the DD reaction cross-sections. When $Y_{tot} \approx Y_{DT}$ the response at S-NAS will be higher than in the case $Y_{tot} \approx Y_{DD}$ because 14 MeV neutrons are more penetrating in the in-vessel structures than 2.5 MeV neutrons (see Fig.2). The amount of variation for Y_{tot} with Y_{DT}/Y_{DD} would depend on the location of S-NAS; it can be evaluated by numerical analyses

and validated by the initial cross calibration measurements with DD operation, and later confirmed by subsequent measurements.

In the case of DEMO or a power plant, the cross calibration factors between S-NAS and L-NAS will also depend on the evolving composition of the Tritium breeding blankets, especially in the case of a solid blanket based on the use of beryllium and lithium ceramic composites. In this case, the burn-up of ^{6}Li in time changes the shielding properties of blankets. For this case, an opportune position of S-NAS will have to be found to reduce this effect.

The full development of this method requires the selection of dosimetry cross-sections and of the cross calibration procedure. It should be developed and tested in ITER in parallel to the current calibration strategy, as it could prove to be the only feasible option in DEMO and in a power plant.

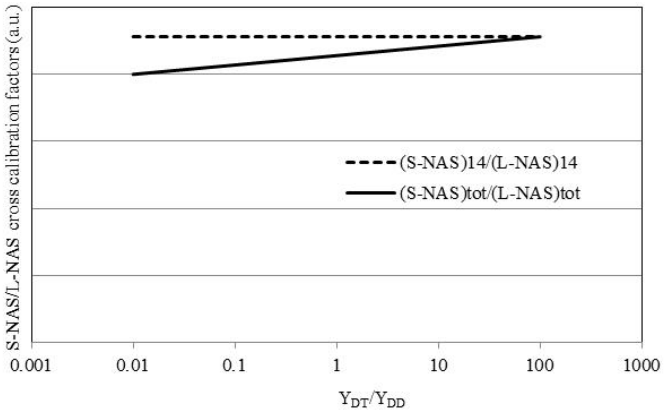

Fig. 2 Cross calibration factors for Y_{tot} and Y_{DT} between S-NAS and L-NAS as a function of Y_{DT}/Y_{DD}

3. Testing in ITER

In the following we investigate the feasibility of testing the proposed method in ITER. The activation reactions producing long-lived isotopes identified for this study are given in Table 1, together with the relevant decay data. These do not exhaust the number of potential reactions that could be used, the purpose here is to show that at least these reactions exist and are available for the purpose.

3.1 Activation reactions

The cross sections of selected reactions are listed in Table 1 and shown in Fig.3 [11]. The reactions identified for DT neutrons have high energy threshold (in the range 5 to 10 MeV), and two reactions are also given in with lower energy thresholds, as the first neutrons will be produced at 2.5 MeV energy by DD plasmas. The use of the ^{59}Co(n,γ)^{60}Co thermal neutron reaction is discussed later. The materials selected are metals with melting temperatures > 1200 °C.

The selection has been done considering the ITER case and the related research plan [12], which foresees a pre-nuclear shutdown, more than one year operation with Deuterium plasma and an initial low duty cycle Deuterium - Tritium operation ending with a short Q=10 pulse, followed by a shutdown. Therefore in ITER an initial dedicated calibration phase would not be possible. This first phase would be followed by full DT operations lasting more than one year. The principle of the method proposed here does not depend on the details of the operation plan, provided that the L-NAS foils could be

installed before and retrieved shortly after nuclear operation phases (within a few months), and this is repeated periodically. In principle, both the Y_{tot} and the Y_{DT}/Y_{DD} could be measured employing different reactions with different energy thresholds. In the ITER case, we consider the second, full DT case as neither Y_{tot} nor Y_{DT}/Y_{DD} are defined yet for the first phase. However, based on the results obtained for a full DT phase, the feasibility of the method for DD operations will be evaluated.

We have considered the DT neutron flux density spectrum at the ITER first wall at the outboard midplane (Fig.4) as a typical position for the L-NAS. In the case of ITER, the L-NAS could be embedded on diagnostics retractable tubes in the equatorial port plugs for the purpose of testing the method. Fig.4 shows also the DT neutron spectrum between the blanket and vacuum vessel (rear blanket) at midplane, where the S-NAS could be located. In the following discussion, these spectra are considered as representative also of DT neutrons generated by triton burn-up in pure DD plasmas, although this is not rigorously correct. Moreover, it has been tentatively assumed that during the full DT phase, lasting 15 months, a total of 2500 DT discharges are performed with an increasing number of DT neutrons produced with two different time profiles given in Fig. 5. In both cases, the DT production starts at zero and reaches the 2.24×10^{20} n/s (Q=10) level at the end of the campaign, and the total DT neutron production is 1.5×10^{25} neutrons.

The calculated specific activities for Ni, Mn, Co and Fe foils irradiated on ITER outboard first wall during the initial low duty cycle DT campaign are shown in Figures 6-9. Only the main activated nuclei are shown. In some cases, the specific activities are given for the two different irradiation scenarios to show the sensitivity to the irradiation scenario. For example, in the case of Nickel foils, the ratio of activities of ^{57}Co to ^{58}Co at end of irradiation is 0. 44 in case b) and 0.54 in case a).

Table 1- Main parameters of selected activation cross sections

Activation reaction	Half life of daughter nuclide	Isotopic abundance of parent nuclide	E_{th} - Energy threshold / Cross section	Energy of gamma emitted (MeV) / Probability
^{60}Ni(n,p)^{60}Co	5.271 y	26.223%	5 MeV /0.15b	1.332 / 99.98 %
^{55}Mn(n,2n)^{54}Mn	312.12 d	100%	10MeV/ 0.5	0.835 / 100%
^{58}Ni(n,d)^{57}Co	271.74 d	68.077%	9 MeV / 0.07	0.122 / 85.6 %
^{59}Co(n,2n)^{58}Co	70.86 d	100%	11 MeV / 0.7 b	0.8108 / 99%
^{54}Fe (n,p)^{54}Mn	312.12 d	5.845%	1.8 MeV/ 0.04	0.251 / 100%
^{56}Fe (n,p)^{56}Mn	2.579 h	91.754%	~1.8 MeV / 0.06b	0.846/98.85%
^{58}Ni (n,p)^{58}Co	70.86 d	68.077%	~1.5 MeV / 0.1b	0.810/ 99.45%
^{59}Co(n,γ)^{60}Co	5.2710 y	100%	-/-	1.332/ 99.98%

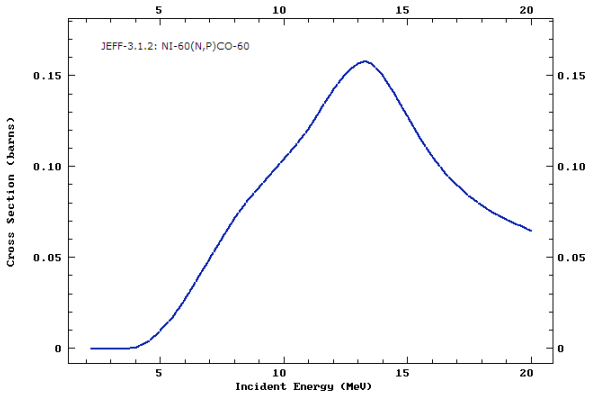

Cross section of $^{60}Ni(n,p)^{60}Co$ reaction

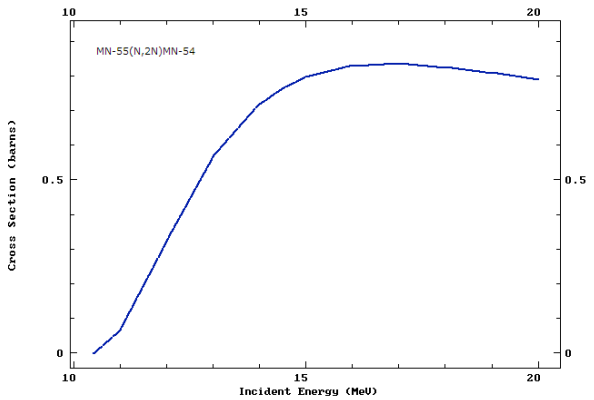

Cross section of $^{55}Mn(n,2n)^{54}Mn$ reaction

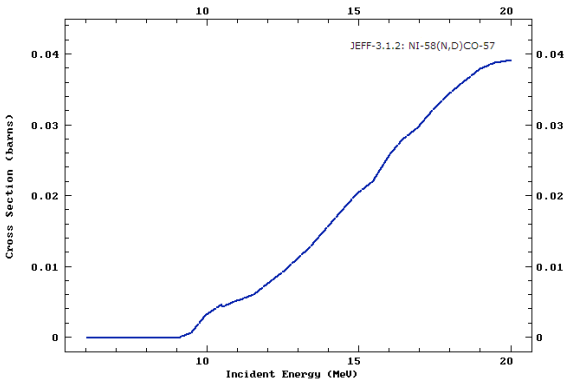

Cross section of $^{58}Ni(n,d)^{57}Co$ reaction

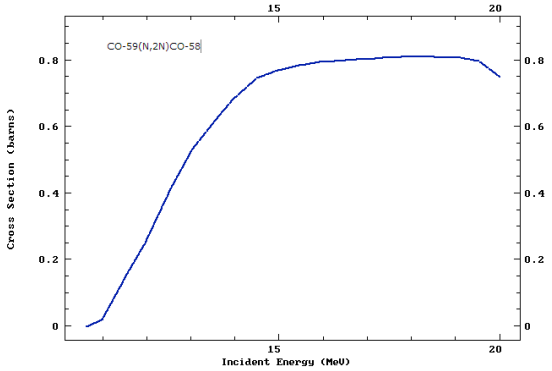

Cross section of $^{59}Co(n,2n)^{58}Co$ reaction

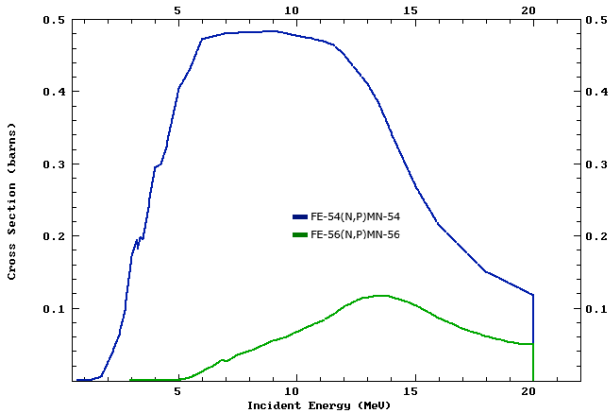

Cross sections of $^{54}Fe(n,p)^{54}Mn$ and $^{56}Fe(n,p)^{56}Mn$ reactions

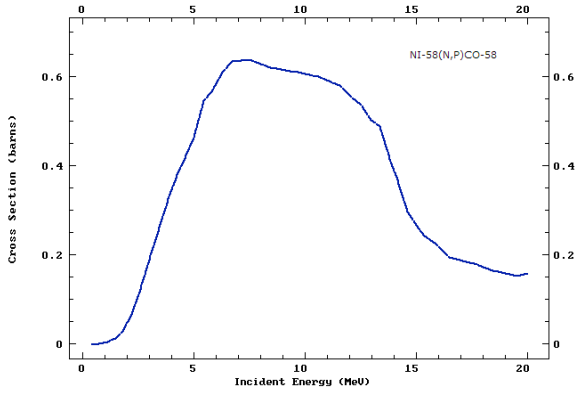

Cross section of $^{58}Ni\ (n,p)^{58}Co$ reaction

Fig.3 Cross section of reactions listed in Table 1

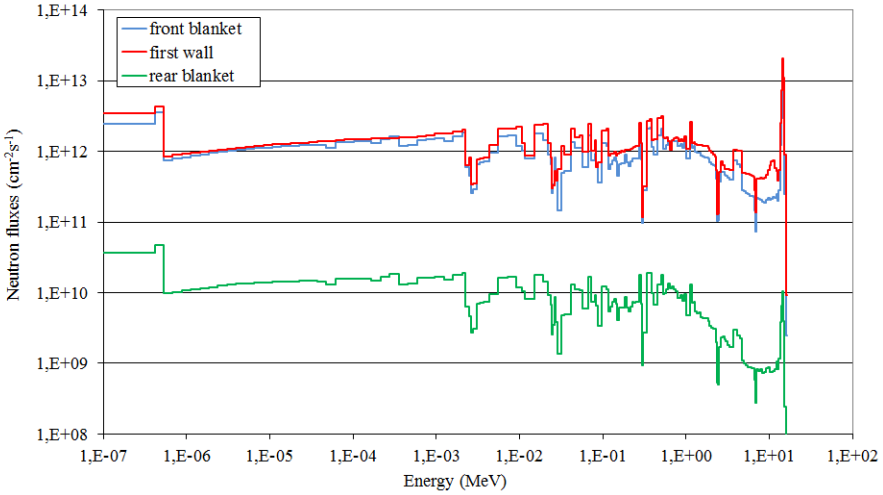

Fig. 4 Energy spectrum of neutron flux density on ITER outboard first wall, front blanket and between blanket and vacuum vessel (rear blanket) at midplane (MCNP output in neutrons per energy bin)

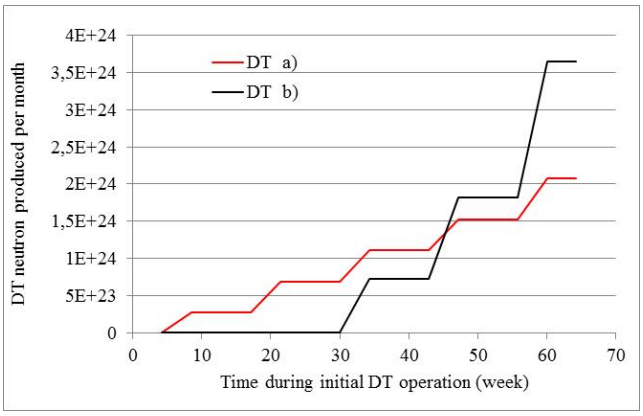

Fig. 5 DT yield distributions during the initial low duty DT operations at ITER

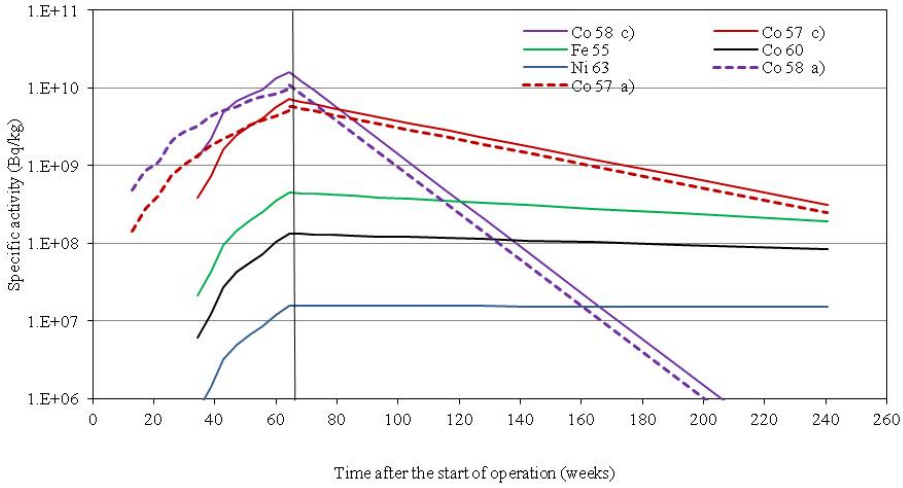

Fig. 6 Specific activity in Nickel foils irradiated on ITER outboard first wall during the initial low duty cycle DT campaign. Only the main activated nuclei are shown. The specific activities of ^{57}Co and of ^{58}Co are shown for two different irradiation scenarios

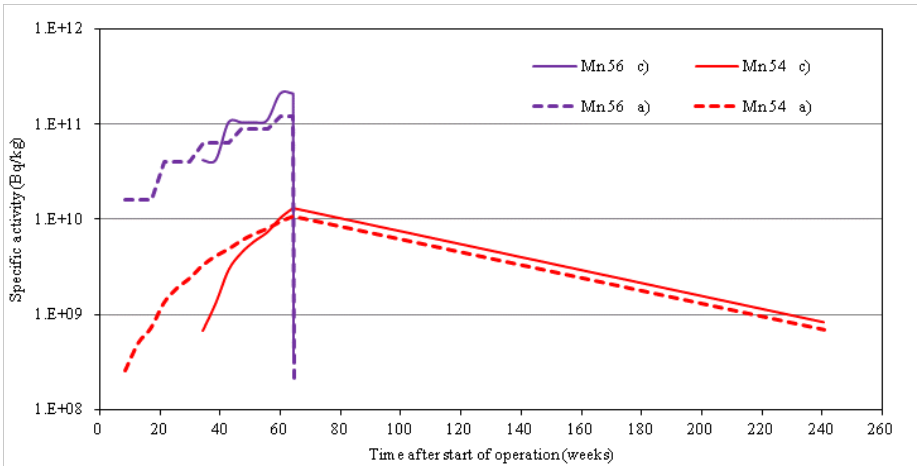

Fig. 7 Specific activity in Manganese foils irradiated on ITER outboard first wall during the initial low duty cycle DT campaign. Only the main activated nuclei are shown. The specific activities of ^{56}Mn and of ^{54}Mn are shown for two different irradiation scenarios

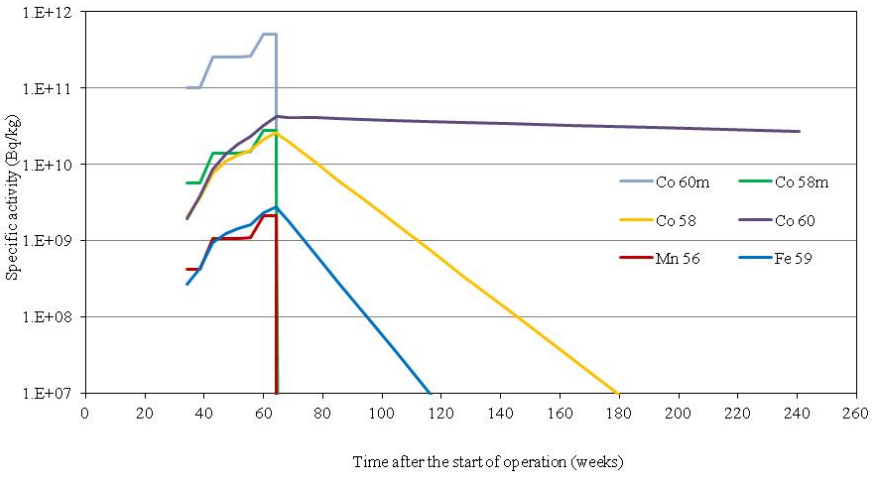

Fig. 8 Specific activity in Cobalt foils irradiated on ITER outboard first wall during the initial low duty cycle DT campaign. Only the main activated nuclei are shown.

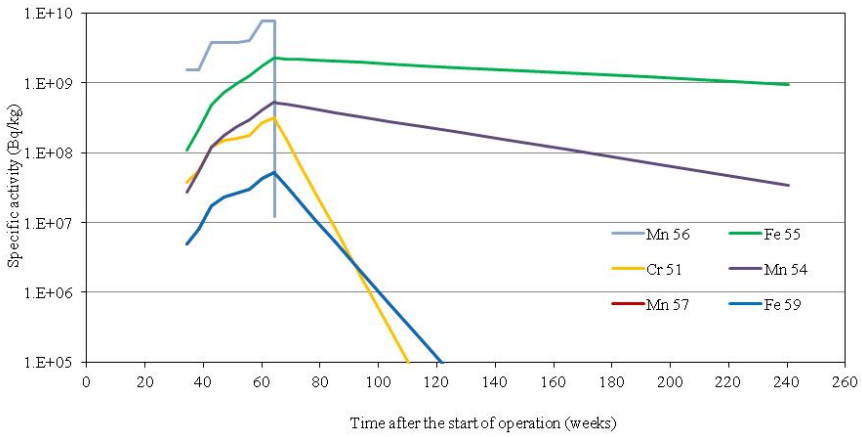

Fig. 9 Specific activity in Iron foils irradiated on ITER outboard first wall during the initial low duty cycle DT campaign. Only the main activated nuclei are shown.

3.2 Discussion

The main advantage of the proposed method is that it can be applied to a wide neutron emission range with a careful choice of sample mass (which could vary from ≈ 0.01 to ≈10 g), counting time and detector efficiency. However, different scenarios have to be considered:

1. DT plasmas - In the investigated scenario, with 1.5 x 10^{25} DT neutrons produced in 15 months, 0.01g foils irradiated in the L-NAS would present activities in the range 10^4 – 10^5 Bq resulting in about 10^2 – 10^3 c/s for a typical HPGe gamma detector. In case the S-NAS is located at the vacuum vessel, the fast neutron flux at the irradiation ends can decrease by about 3 orders of magnitude as compared to the first wall (Fig.4). Therefore, 1 g samples would present about 10 – 10^2 c/s and would easily provide very accurate measurements. L-NAS in DT would provide a calibration of neutron monitors with practically no minimum requirement on the neutron yield. Cross calibration of L-NAS and S-NAS would require a minimum yield of about 10^{21} - 10^{22} neutrons (assuming that a minimum counting rate > ≈ 0.1 c/s is typically needed for the activity measurement).

2. DT from triton burnup in DD plasmas - In this case, taking into account that neutron yields from Deuterium plasmas are typically 200 times smaller than from equivalent DT plasmas, and that the triton burnup is a few times 10^{-2}, the DT yields would be typically 10^4 lower than in the previous case 1. For reactions induced by 14 MeV neutrons, 1g foils irradiated in the L-NAS would present activities in the range 10^2 – 10^3 Bq resulting in about 1 - 10 c/s for a typical HPGe gamma detector. L-NAS would provide accurate measurements of Y_{DT} with yields > ≈ 10^{21} neutrons. In case the S-NAS, 10 g foils would still provide 0.1 c/s in case of the most active reactions. Note that samples can be removed from S-NAS immediately after the end of irradiation. A minimum DT yield from triton burnup is therefore needed to cross calibrate the L-NAS and the S-NAS, corresponding to a minimum DD yield of about 10^{23} neutrons. This value is derived in the assumption that the same reactions are used for L-NAS and S-NAS, and would depend on the exact position of S-NAS. However, for the purpose of cross calibrating the L-NAS and the S-NAS, other reactions could be used in S-NAS, characterized by much higher cross section values, such as the $^{59}Co(n,\gamma)^{60}Co$ reaction shown in table I. The use of this reaction would decrease the minimum neutron yield by about one order of magnitude.

3. DD plasmas – In case of DD operations, typically a factor 200 fewer neutrons would be produced than in DT operations. Moreover, only the $^{54}Fe(n,p)^{54}Mn$ and the $^{58}Ni(n,p)^{58}Co$ reactions can be used, and their cross sections at 2.5 MeV are about one order of magnitude lower than at 14 MeV. At L-NAS on the first wall, ^{58}Co and ^{54}Mn products can be expected to present about 10^4 Bq/g and 10^2 Bq/g, providing 10^2 c/s and 1 c/s, respectively, for a one gram mass foil. In S-NAS, larger samples of 10 g would suffice to obtain accurate counting statistics for ^{58}Co. In order to produce statistically accurate measurements in the S-NAS for cross calibration with L-NAS, this minimum DD neutron yield of about 10^{23} neutrons has to be produced in the first nuclear phase devoted to the first neutron calibration. This value would depend on the exact position of S-NAS. Here, again, the use of $^{59}Co(n,\gamma)^{60}Co$ reaction would decrease the minimum neutron yield by about one order of magnitude.

We conclude that the method is feasible for a full DT phase in ITER, with a minimum $Y_{DT} \approx 10^{21}$ - 10^{22} neutrons. For pure DD operations a minimum $Y_{DD} \approx 10^{23}$ neutrons is required (e.g., in ITER: 2500 discharges of 400 s, each producing 10^{17}n/s). In case the $^{59}Co(n,\gamma)^{60}Co$ reaction is used in the S-NAS for cross calibration with the L-NAS, a minimum $Y_{DD} \approx 10^{22}$ neutrons is required. In this case the method could possibly be tested also during the first ITER nuclear phase.

The feasibility of measurements after short irradiations in the S-NAS (for monitoring the temporal stability of neutron monitors) is not expected to be an issue and is not discussed here. We only note that activation measurements using reactions producing short-lived radionuclides are routinely carried out on a shot-by-shot basis in DD and in DT operations at JET where the local neutron flux at the NAS is comparable to that expected in a potential S-NAS in ITER [13].

There are however other potential issues which are addressed in the following.

Availability of suitable locations Provided that the activation foils are exposed in L-NAS in locations sufficiently close to the first wall, and high energy threshold activation reactions are used, the activation system can be considered to respond mostly to direct neutrons, with numerical calculations relating the total neutron source to the local fluence, thus providing also the contribution due to scattered neutrons (the effect of plasma position is discussed below). The advantage of the method therefore relies on the possibility to install the foils in positions suitable and accessible periodically (every few years). These could be found in blanket shield modules, i.e. behind or in the first wall panels of port plugs which are to be removed when maintenance is required. Small samples and holders would be attached (by welded attachments) with no need of a separate cooling loop.

Sensitivity to plasma displacements or plasma shape If the activation foils are exposed in L-NAS close to the first wall, and high energy threshold activation reactions are used, we may expect that the resulting activation depends on the plasma position and, on a lower extent, on its shape. In order to quantify this effect, we calculate the flux Φ at a given position on the outboard first wall at midplane, where the foils are located, from a ring neutron source of unitary intensity located at $R=R_r$ on the midplane at a distance a_r from the outboard wall (Fig. 10), with $R_r + a_r = R_0 + a$, where R_0 is the major radius, and a is the horizontal minor radius (in ITER $R_0 = 6$m and a = 2m). The ring source simulates the highly peaked neutron emission.

The flux at the foil position is given by

$$(R_r, a_r) = \frac{1}{2\pi} \int \frac{d}{d^2} = \frac{1}{2\pi} \int \frac{d}{R_r^2 \sin^2 + (a_r + R_r - R_r \cos)^2} =$$

$$(R_r, a_r) = \frac{1}{2\pi} \int \frac{d}{R_r^2 + (a_r + R_r)^2 - 2R_r(a_r + R_r)\cos}$$

$$(R_r, a_r) = \frac{1}{4\pi R_r (a_r + R_r)} \int \frac{d}{k - \cos}$$

$$(R_r, a_r) = \frac{1}{4\pi R_r (a_r + R_r)} \left| \frac{2 \tan^{-1} \frac{(k+1)\tan\frac{}{2}}{\sqrt{k^2 - 1}}}{\sqrt{(k^2 - 1)}} \right| = \quad (9)$$

$$k = \frac{R_r^2 + (a_r + R_r)^2}{2R_r(a_r + R_r)} = 1 + \frac{a_r^2}{2R_r(a_r + R_r)} > 1$$

where we have taken into account that the angles in the intervals $-\pi<\alpha<-\beta$ and $\beta<\alpha<\pi$ are shielded by the central column. The angle β depends on the tokamak aspect ratio ($\beta\sim 110°$ in ITER).

The variation of the neutron flux at the foil position at varying $R_r + a_r$ resulting from Eq.(9) is shown in Fig. 11 as a function of $R_r - R_0$. Variations of +10% (-10%) in the distance of the ring from the ouboard wall causes ~10% variation in the fluence at the foils located on the outboard midplane. These results are in line with the sensitivity analysis presented in [8]. These variations would be detected and then taken into account in the calculation of the local neutron fluence at L-NAS. They could also be detected using several foils located in other poloidal positions, resulting in a reduction of the uncertainty due to the plasma position to <<10%. On the other hand, this uncertainty should be compared with that introduced by using in-vessel a large neutron generator as a calibrating source, deployed by remote handling. In this case both the uncertainty on the absolute neutron emission from the generator and on its angle-energy distribution would hardly be much less significant.

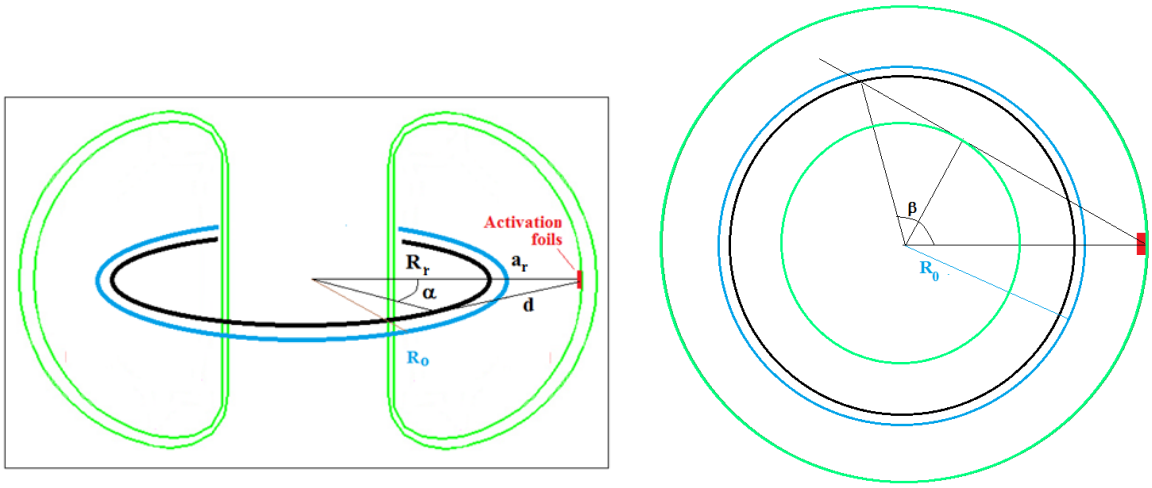

Fig.10 Schematic view of ring source located at $R=R_r$ on the midplane at a distance a_r from the outboard wall.

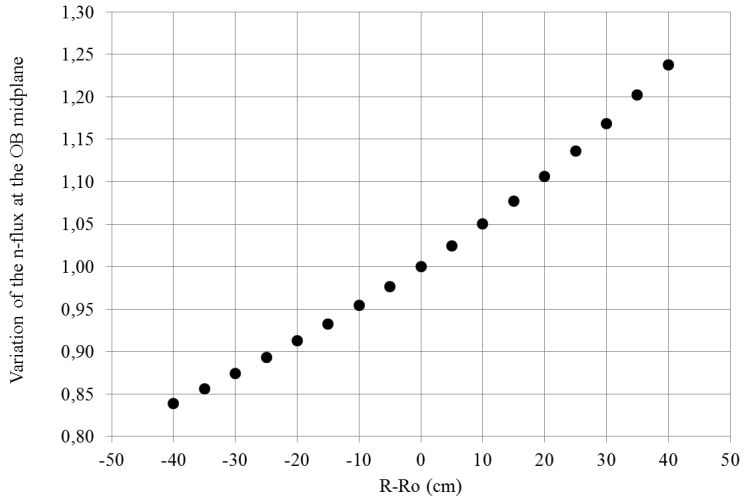

Fig 11 Variation of the flux at on the outboard first wall at midplane, where the foils are located, from a ring neutron source of unitary intensity as a function of $R_r - R_0$, with $R_0 = 6m$ and $a = 2m$ (as in ITER).

Sensitivity to neutron energy spectrum The shape of the neutron spectrum in the fusion peak depends on the presence of auxiliary heating, on the nature of the auxiliary heating itself (rf waves or neutral particle beams), and on its energy. Changes in the neutron spectrum at energies above the energy threshold of the selected activation reactions in the L-NAS can result in changes of the induced activities in activation foils with fixed local neutron fluence. If the neutron spectrum is measured and known, these effects can be easily taken into account. If the spectrum is not measured, but only calculated, the sensitivity of the method to changes of the energy spectrum can be evaluated and minimized by i) using reactions with almost flat cross section at around 14 MeV (if available), and ii) by using different reactions and unfolding the neutron spectrum from multifoil activation analysis method.

Accuracy of neutronics calculations & cross sections In case suitable irradiation location could be found close to the first wall for L-NAS, and high energy threshold activation reactions are used, the activation results mostly from direct neutrons. The uncertainties due to the neutron transport calculations would be small and would provide a limited contribution to the total uncertainty on the measurement. Moreover, they should be compared with those introduced by using a large neutron generator as a calibrating source. The activation cross sections considered in Table 1 are all established dosimetric reactions (with the exception of the $^{58}Ni(n,d)^{57}Co$) whose cross sections are accurately known [11,14]. However, a dedicated programme of cross section validation could be carried out if needed. In time, the L-NAS combined with S-NAS would serve as a periodic check of the calibration of the neutron detector system with increasing accuracy.

Other sources of uncertainties in the proposed method are common to the usual calibration approach.

6. Proposed test in JET in DD and DT operations

The use of activation reactions leading to long lived nuclides is new in fusion research were short-lived nuclei have been preferred for reasons explained above. The reactions considered here have never been used before in fusion facilities, except in the case of the first Deuterium-Tritium campaign at JET in 1997 [15]. JET has full capability of operating with Tritium and it is the only fusion machine capable of producing significant neutron yields, typically $\approx 10^{16}$ n/s (2.5 MeV) in DD and up to nearly 10^{19} n/s (14.1MeV) in DT operations. A second Deuterium-Tritium campaign is planned at JET in 2019. The present option for the DT experiments (DTE2, after DTE1 performed in 1997) is to use the full budget of 1.7×10^{21} neutrons still available to JET. This proposed 14MeV neutron budget is nearly an order of magnitude higher than any previous DT campaigns (JET or TFTR). The calculated neutron fluence on JET first wall at the end of DTE2 will be up to10^{20} n/m^2, a level that is hardly achievable at existing 14 MeV neutron generators. A new calibration of JET neutron detectors at 14 MeV neutron energy is also being prepared, using a DT neutron generator deployed at different toroidal/poloidal positions inside the vacuum vessel [5]. Both the external fission chambers and the internal activation system (a sort of S-NAS) will be absolutely calibrated.

Moreover, for the purpose of investigating the neutron induced activation in ITER real materials, two sample holders have been installed on the JET first wall (a sort of L-NAS), each one containing 60 1-mm thick, 18-mm diameter activation foils, with the purpose of measuring the local neutron fluence and spectrum (Figures 12 and 13). For this purpose a number of different dosimetry foils have been located and will be exposed in the next DD campaign. Dosimetry foils will also be irradiated in the following DT campaign together with samples of the real ITER materials. The foils will be retrieved after each campaign and the total neutron yields produced by JET will also be derived from the measurements of their activity. The activation reactions that will be used are listed in Table 2. The combination of the recent 2.5 MeV calibration, the new 14 MeV calibration using a neutron generator and the use of the L-

NAS in JET will offer an unique opportunity for comparing the new calibration approach proposed here with the traditional one.

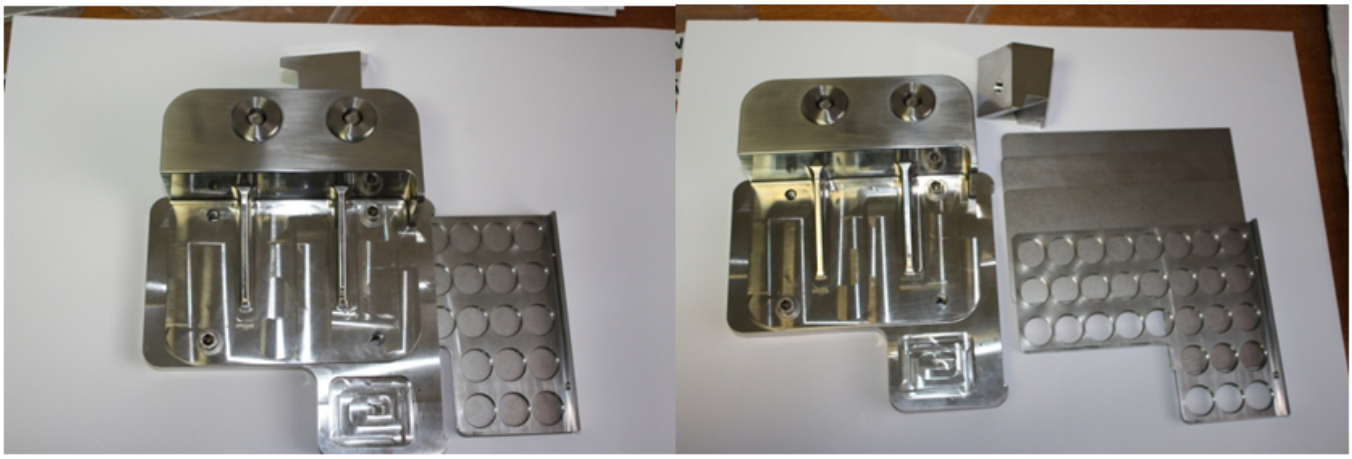

Fig.12 One of the 2 sample holders of the Long Term Irradiation Station (LTIS) to be installed in JET Oct.4 & 8

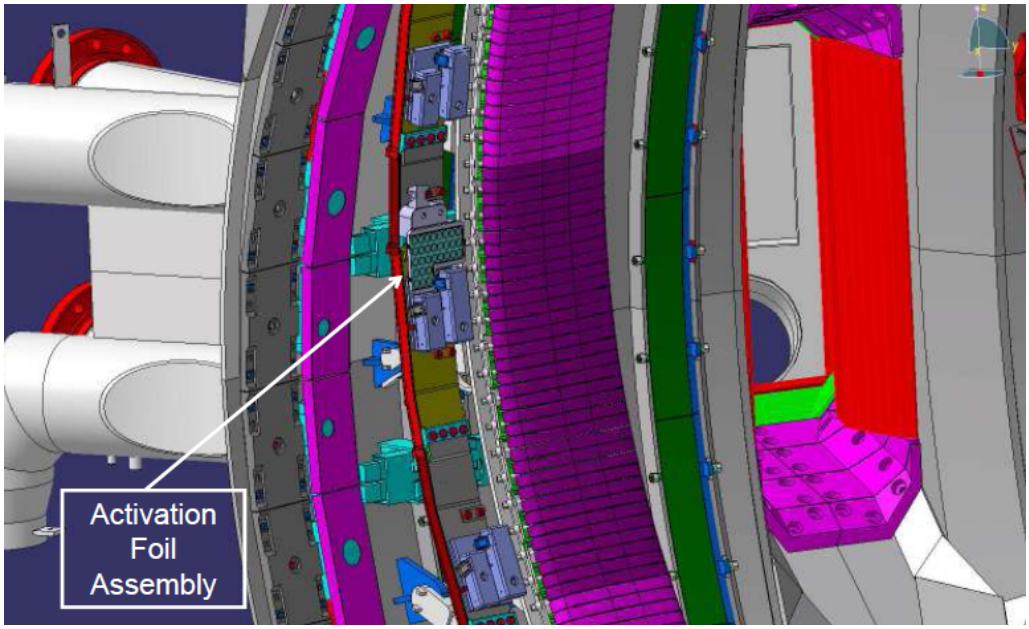

Fig.13 Sample holder installed inside JET close to the first wall

Table 2 – Activation reactions used in the JET activation measurements on the first wall (L-NAS)

Activation reaction	Half-life of daughter nuclide	Isotopic abundance of parent nuclide	Energy threshold (MeV) / Cross section (b)	Gamma emitted (MeV) / Probability	Melting temp. (°C)
14 MeV (DT or from triton burnup in DD)					
$^{48}Ti(n,p)^{48}Sc$	83.8 d	8.25%	3.8 / 0.29	0.889 / 99.98%	1668
$^{55}Mn(n,2n)^{54}Mn$	312.12 d	100%	10.5 / 0.68	0.835 / 99.98%	1244
$^{59}Co(n,2n)^{58}Co$	70.86 d	100%	10.7 / 0.69	0.811 / 99%	1495
$^{60}Ni(n,p)^{60}Co$	1925.28 d	26.223%	5 / 0.15	1.173 / 99.97% 1.332 / 99.99%	1455
$^{89}Y(n,2n)^{88}Y$	106.63 d	100%	11.6 / 0.82	1.836 / 99.2% 0.898 / 93.7%	1526
2.5 MeV					
54Fe(n,p)54Mn	312.12 d	5.845%	1.8 / 0.05	0.835 / 99.98%	1538
$^{58}Ni(n,p)^{58}Co$	70.86 d	68.077%	1.5 / 0.1	0.811 / 99%	1455
Thermal					
$^{59}Co(n,\gamma)^{60}Co$	1925.28 d	100%	Well established dosimetry reactions	1.173 / 99.97% 1332 / 99.99%	1495
$^{45}Sc(n,\gamma)^{46}Sc$	83.8 d	100%		0.889 / 99.98%	1539
$^{58}Fe1.332(n,\gamma)^{59}Fe$	44.5 d	0.282%		1.099 / 56.5%	1538
$^{181}Ta(n,\gamma)^{182}Ta$	115 d	99.988%		0.068 / 41.2%	3017

4. Conclusions

An original approach for the calibration of neutron detectors in DEMO and fusion power plants is presented in this paper, which originates from the experience gained on existing fusion devices, mainly JET, and is motivated by the recognition of the increasing difficulties of obtaining such calibration with the required accuracy in ITER and DEMO.

This approach is entirely based on the use of the neutron activation method and aims at providing a periodic calibration of active neutron detectors along the reactor lifetime. It employs activation reactions generating both short and long-lived radioisotopes, with activation samples irradiated both close to the first wall, from which the absolute calibration is derived, and at the vacuum vessel. These last ones would "bridge" the calibration factors to external monitors by also providing a control of their stability in time. This proposed solution disentangles the problem of accurate absolute calibration from the time resolved measurement of fusion power, and requires a first, dedicated nuclear phase of operations devoted to calibration of the activation system at the beginning of the reactor life.

Various sources of uncertainties are discussed, such as due of changes in plasma position, neutron energy spectrum, and due to uncertainties in neutron transport and dosimetric cross sections. These are compared with uncertainties introduced by the use in-vessel of large DT neutron generators (accelerators) deployed by remote handling in the traditional calibration procedures.

The feasibility of the proposed approach has been investigated considering the ITER case for which suitable reactions have been identified and the expected activity levels have been calculated. It has been shown that testing the method in ITER is feasible in the second, full DT with a minimum $Y_{DT} \approx 10^{21}$ - 10^{22} neutrons. For a pure, DD operations a minimum $Y_{DD} \approx 10^{23}$ neutrons would be required. In

case the $^{59}Co(n,\gamma)^{60}Co$ reaction is used in the S-NAS for cross calibration with the L-NAS, a minimum $Y_{DD} \approx 10^{22}$ neutrons would be required. In this case the method could possibly be tested also during the first ITER nuclear phase. All results presented, however, depend on the availability of suitable locations for both the L-NAS and the S-NAS, and are subject to the verification of the activation calculation for such specific locations.

In the frame of JET technology program, two sample holders have been installed on the JET first wall (a sort of L-NAS). A number of different dosimetry foils have been located in these holders and will be exposed in the next DD and DT campaigns with the purpose to measure the local neutron fluence. A number of different activation reactions producing long-lived radioisotopes are employed. After the retrieval of foils at the end of experimental campaigns, the neutron-induced activity will be measured and the total neutron yields will then be derived from this measurement. The combination of the new planned 14 MeV neutron calibration using a neutron generator and the use of the L-NAS in JET will offer an unique opportunity for comparing the new calibration approach proposed here with the traditional one.

Acknowledgements

This work has been carried out within the framework of the EUROfusion Consortium and has received funding from the Euratom research and training programme 2014-2018 under grant agreement No 633053. The views and opinions expressed herein do not necessarily reflect those of the European Commission.

References

[1] O.N. Jarvis, G. Sadler, P. van Belle, T. Elevant, In vessel calibration of JET neutron monitors using a ^{252}Cf neutron source: difficulties experienced, review of Scientific Instruments 61,

[2] J.D.Strachan et al., Neutron calibration techniques for comparison of tokamak results, Review of Scientific Instruments 61, 10 (1990)

[3] M. Angelone, P. Batistoni et al., Calibration of the neutron activation system on the Frascati Tokamak Upgrade: comparison between measured and calculated activation response coefficients, Fusion Technology, 19 (1991)

[4] D.B. Syme, S Popovichev, S Conroy, I Lengar, L Snoj, C Sowden, L Giacomelli, G Hermon, P Allan, P Macheta, D Plummer, J Stephens, P Batistoni, Mr R. Prokopowicz, S. Jednorog, MR Abhangi, R Makwa, The JET Neutron Calibration 2013 and its Results, Fusion Engineering and Design, Volume 89, Issue 11, November 2014, Pages 2766-2775 ISSN: 0920-3796

[5] P. Batistoni, D. Campling, D. Croft, S. Conroy, T. Giegerich, T. Huddleston, X. Lefebvre, I. Lengar, S. Lilley, M. Pillon, A. Peacock, S. Popovichev, S. Reynolds, R. Vila, R. Villari, N. Bekris, Technological exploitation of Deuterium-Tritium operations at JET in support of ITER design, operation and safety, submitted to Fusion Engineering Design

[6] L. Bertalot, R. Barnsley, M.F. Direz, J.M. Drevon, A. Encheva, S. Jakhar, Y. Kashchuk, K.M. Patel, A.P. Arumugam, V. Udintsev, C. Walker and M. Walsh, Fusion neutron diagnostics on ITER tokamak, Journal of Instrumentation, Volume 7 (2012)

[7] M. Sasao, L. Bertalot, M. Ishikawa and S. Popovichev. Strategy for the absolute neutron emission measurement on ITER. Rev. Sci. Instrum. 81, 10D329 (2010)

[8] M. SASAO, M. ISHIKAWA, G. YUAN, K. PATEL, S. JAKHAR, Y. KASHCHUK and L. BERTALOT, Issues on the Absolute Neutron Emission Measurement at ITER, Plasma and Fusion Research: Regular Articles Volume 8, 2402127 (2013)

[9] T. Nishitani, K. Ebisawa, S. Kasai, and C. Walker, Neutron activation system using water flow for ITER, Review of Scientific Instruments 74, 1735 (2003)

[10] U. Fischer, M.Angelone, T. Bohm, K. Kondo, C. Konno, M. Sawan, R. Villari, B. Walker, Benchmarking of FENDL-3

Neutron Cross-section Data Starter Library for Fusion Applications, Nuclear Data Sheets, june 2014, 120:230-234.

[11] Eva M. Zsolnay, Roberto Capote Noy, Henk J. Nolthenius, Andrej Trkov, Summary Description of the New International Reactor Dosimetric and Fusion File (IRDFF release 1.0), INDC(NDS)-0616.

[12] D.J. Campbell, IAEA Fusion Energy Conference, San Diego, 9.10. 2012, https://www.iter.org/doc/www/content/com/Lists/Stories/Attachments/1361/David2.pdf

[13] R. Prokopowicz, B. Bienkowska, K.Drozdowicz, S.Jednorog, E. Kowalska-Strzeciwilk, A. Murari, S. Popovichev, K. Pytel, M. Scholz, A. Szydlowski, B. Syme, G. Trac, Nuclear Instruments and Methods in Physics Research A 637 (2011) 119-127

[14] G. Stankunas, P. Batistoni, S. Conroy, Activation cross sections for DD, DT and TT neutrons from JET plasmas, Final Report of Task EFDA - JET Fusion Technology JW12-FT-5.54

M. J Loughlin, R. A Forrest, J. E. G Edwards, Neutron activation studies on JET, Fusion Engineering and Design 2001; 58, 967-9

Fig 10b: Variation of the flux at on the outboard first wall at midplane, where the foils are located, from a ring neutron source of unitary intensity as a function of R_r - R_0, with R_0 = 6m and a = 2m (as in ITER).

[15] ù